Electrodynamics analysis on coherent perfect absorber and phase-controlled optical switch

Tianjie Chen,[1] Shaoguang Duan,[2] and Y. C. Chen[3,*]

[1]*Palm Springs International Garden, A-6262, Chongqing 401121, China*
[2]*College of Physics, Chongqing University, Chongqing, 400030, China*
[3]*Department of Physics and Astronomy, Hunter College of the City University of New York, 695 Park Avenue, New York, New York 10065, USA*
**Corresponding author: y.c.chen@hunter.cuny.edu*

Received October 4, 2011; revised January 19, 2012; accepted January 19, 2012;
posted January 19, 2012 (Doc. ID 155905); published April 11, 2012

A coherent perfect absorber is essentially a specially designed Fabry–Perot interferometer, which completely extinguishes the incident coherent light. The one- and two-beam coherent perfect absorbers have been analyzed using classical electrodynamics by considering index matching in layered structures to totally suppress reflections. This approach presents a clear and physically intuitive picture for the principle of operation of a perfect absorber. The results show that the incident beam(s) must have correct phases and amplitudes, and the real and imaginary parts of the refractive indices of the media in the interferometer must satisfy a well-defined relation. Our results are in agreement with those obtained using the *S*-matrix analysis. However, the results were obtained solely based on the superposition of waves from multiple reflections without invoking the concept of time reversal as does the *S*-matrix approach. Further analysis shows that the two-beam device can be configured to function as a phase-controlled three-state switch.

OCIS codes: 120.2230, 030.1670, 230.1150, 230.3750, 260.2160.

1. INTRODUCTION

A coherent perfect absorber (CPA), or antilaser, is a device that absorbs coherent light and converts it into heat or other forms of internal energy [1]. It is the time-reversed counterpart of a laser [2]. The concept was first presented by Chong *et al.* [3]. Recently, the first working model capable of absorbing 99.4% of all incident light was reported [4]. The device was a two-channel CPA device that absorbed two incident laser beams when the beams had the correct phases and amplitudes. It was predicted that if a good source laser were available, the absorption could reach 99.999%.

A laser is a Fabry–Perot resonator filled with an active material that can convert the stored energy into coherent light [5]. In recent years, a scattering *S*-matrix approach, which was originally used in elementary particle physics, was introduced into laser physics [3]. Furthermore, the concept of time reversal, first applied to light-matter interactions in the 1950s, is the basis of spin echoes and photon echoes [6,7]. More recently, Chong *et al.* [3], based on the scattering *S*-matrix approach and the concept of time reversal, proposed a time-reversed lasing process, which has led to a new device as a counterpart of the laser. The device was named as an "antilaser" or a "time-reversed laser." This device may absorb the incident coherent light completely and, therefore, it is also called a CPA [3].

The scattering *S*-matrix approach is basically a mathematical approach used in theoretical physics. It is somewhat inconvenient to use as a tool for device designer. Tsien [8] pointed out that it is all the more true when one realizes that the mathematical difficulties of any subject are usually quite artificial and, with a little interpretation, the matter could generally be brought down to the level of a research engineer. In this paper, an electrodynamics approach, which is simply based on the superposition of multiple reflected waves similar to the way the single- and multiple-layer optical coatings are treated, is used to analyze the behavior of the one-beam, two-beam CPAs, as well as the three-state phase-controlled optical switch.

There are various types of laser resonators. As far as the physical structure is concerned, most lasers have a one-sided structure, in which a laser beam is emitted from one of the end mirrors of the resonator and not from the other, which is a total reflector. There are also two-sided lasers, such as the uncoated diode lasers, whose output beams are emitted symmetrically from both ends of the resonator. As the counterpart, there exist two types of CPAs: the one-beam CPA, which completely absorbs an incident coherent beam, and the two-beam CPA, which completely absorbs two counterpropagating incident coherent beams. Our results show that, in order to extinguish the incoming coherent beams, the real and imaginary parts of the refractive indices of the media in the interferometer must satisfy a well-defined relation, and in the two-beam CPA, the two incident beams must also have correct relative phases and amplitudes. Our results are in agreement with those obtained using the *S*-matrix analysis [3]. The analysis for the one-beam CPA is of particular interest not only because the one-beam device is simpler to analyze and to make, but also because the analysis helps reveal the conceptually simple nature of the CPA. By using the principle of superposition of reflected waves in a layered structure, the one-beam CPA amounts to an antireflection coating on a total reflector with appropriately tailored real and imaginary parts of the refractive indices as well as layer thickness to totally suppress the reflection. Furthermore, the two-beam CPA can

be understood by considering the real and virtual images of the one-beam CPA with respect to a total reflector.

We note that we obtained these results solely based on the superposition of reflected waves from multiple surfaces without invoking time reversal as does the *S*-matrix approach. For a given interferometer length, the occurrence of CPA requires the absorption coefficient to satisfy a well-defined relation, which gives a critical value and not a threshold value as commonly understood in laser physics. This point will be discussed in Section 2.

2. TWO-BEAM CPA

Born and Wolf [9] presented a comprehensive analysis on a symmetrical Fabry–Perot interferometer consisting of a nonabsorbing medium sandwiched between two reflecting mirrors for a single incident beam. In a two-beam coherence perfect absorber, the Fabry–Perot structure is filled with an absorbing medium with two partially transmitting end surfaces, and two counterpropagating coherent light beams are separately incident on both end surfaces. Figure 1 illustrates such a two-beam Fabry–Perot interferometer, which can function as a CPA. The device consists of a slab of absorbing medium having a complex refractive index $\tilde{n}_2 = n_2 + in_{2i}$ and thickness L immersed in a nonabsorbing medium with a real refractive index n_1, which is approximately 1 in air. Two coherent beams, a left beam $I_L^{(i)}$ with electric field $E_L^{(i)}$ and a right beam $I_R^{(i)}$ with electric field $E_R^{(i)}$, are incident on the left and right surfaces, respectively, where $E_L^{(i)}$ and $E_R^{(i)}$ are

$$E_L^{(i)} = \varepsilon^{(i)} e^{-i(\omega t - kz + \varphi_L)} = A_L^{(i)} e^{-i(\omega t - kz)}, \tag{1}$$

$$E_R^{(i)} = \varepsilon^{(i)} e^{-i(\omega t + kz + \varphi_R)} = A_R^{(i)} e^{-i(\omega t + kz)}, \tag{2}$$

where $A_L^{(i)}$ and $A_R^{(i)}$ are complex amplitudes, ω is the angular frequency of light, k is the wave number $k = n_1\,\omega/c$, and c is the speed of light. Hereafter, the subscripts L and R stand for the left and right sides of the interferometer, respectively; and the superscripts (i), (r), and (t) stand for the incident, reflected, and transmitted waves, respectively. We assume that both beams have the same real amplitude $\varepsilon^{(i)}$, polarized in the X-direction, propagating in the $+Z$ or $-Z$ directions, with initial phase factors φ_L and φ_R for the left and right beams, respectively, All vectors are referred to the Cartesian coordinate system defined in Fig. 1.

The problem of a light beam at normal incidence on a Fabry–Perot interferometer filled with a nonabsorbing medium has been treated in [9]. At the first interface, the incident

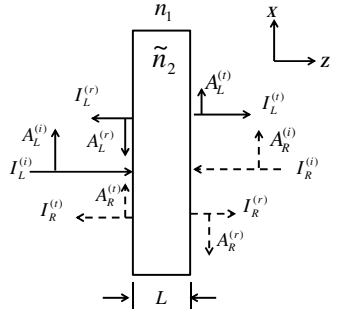

Fig. 1. Fabry–Perot interferometer with two counterpropagating beams incident on the opposite sides of the interferometer.

beam is partially transmitted and partially reflected by the mirror. The transmitted beam subsequently undergoes further reflections and transmissions in multiple round trips in the interferometer. At the left surface, the outgoing beam, propagating in $-Z$ direction as shown in Fig. 1, is the superposition of the reflected beam on the left surface and the transmitted beams originating from the left beam after multireflections, and the transmitted beams originating from the right beam after multireflections. The reflection and transmission coefficients at the left surface are r and t for an external reflection and r' and t' for an internal reflection where the coefficients satisfy the following relations [9]:

$$r = -r' = \frac{n_1 - n_2}{n_1 + n_2}, \qquad t = \frac{2n_1}{n_1 + n_2}, \qquad t' = \frac{2n_2}{n_1 + n_2}, \tag{3}$$

$$tt' + r^2 = tt' + r'^2 = tt' - rr' = 1, \tag{4}$$

where n_1 and n_2 are the real parts of the refractive indices of the surrounding medium and the slab, respectively. For semiconductors, such as silicon, n_2 is dispersive and depends on the doping concentration.

Born and Wolf [9] also showed that as the beam traverses through a nonabsorbing slab, the phase shift δ, after each round trip in the interferometer, is given by $\delta = \frac{4\pi n_2 L}{\lambda_0}$, where λ_0 is the wavelength in free space. When the interferometer is filled with an absorbing medium, an imaginary part of the refractive index must be included and the round-trip phase shift becomes a complex number:

$$\delta = \frac{4\pi \tilde{n}_2 L}{\lambda_0} = \delta_1 + i\delta_2 = \frac{4\pi n_2 L}{\lambda_0} + \frac{i4\pi n_{2i} L}{\lambda_0}, \tag{5}$$

where δ_1 stands for a phase shift caused by the real part of the refractive index n_2 and δ_2 stands for the round-trip absorption caused by the imaginary part of the refractive index n_{2i}.

The electric field of the reflected beam, $E_L^{(r)}$, originating from the left beam, is the sum of the reflected wave on the left surface, and transmitted beams originate from the left beam after multiple reflections in the slab. $E_L^{(r)}$ can be expressed as

$$E_L^{(r)} = \varepsilon_L^{(r)} e^{-i(\omega t + kz + \varphi_L)} = A_L^{(r)} e^{-i(\omega t + kz)}, \tag{6}$$

where $A_L^{(r)}$ is given as [9]

$$A_L^{(r)} = \frac{(1 - e^{i\delta})r}{1 - r^2 e^{i\delta}} A_L^{(i)}. \tag{7}$$

At the left surface, there will be another contribution to the outgoing beam originating from the right beam after multiple reflections in the interferometer, whose electric field is given by

$$E_R^{(t)} = \epsilon_R^{(t)} e^{-i(\omega t + kz + \varphi_R)} = A_R^{(t)} e^{-i(\omega t - kz)}, \tag{8}$$

$$A_R^{(t)} = \frac{tt'}{1 - r^2 e^{i\delta}} A_R^{(i)} e^{i\frac{\delta}{2}}, \tag{9}$$

where the term $e^{i\frac{\delta}{2}}$ representing the phase shift and absorption in a single pass is included to correctly describe the phase

relation between beams originating from the left and right beams.

The total amplitude of the outgoing beam, $A_{\text{Left}}^{(\text{total})}$, propagating towards the left, is the coherent addition of $E_L^{(r)}$ and $E_R^{(t)}$:

$$A_{\text{Left}}^{(\text{total})} = \frac{\varepsilon^{(i)} e^{i\varphi_L}}{1 - r^2 e^{i\delta}} \left[(1 - e^{i\delta}) r + tt' e^{\frac{i\delta}{2}} e^{i\Delta} \right]. \tag{10}$$

Similarly, the total amplitude $A_{\text{Right}}^{(\text{total})}$ of the outgoing beam propagating towards the right is

$$A_{\text{right}}^{(\text{total})} = \frac{\varepsilon^{(i)} e^{i\varphi_R}}{1 - r^2 e^{i\delta}} \left[(1 - e^{i\delta}) r + tt' e^{\frac{i\delta}{2}} e^{i(-\Delta)} \right], \tag{11}$$

where $\Delta = \varphi_R - \varphi_L$.

A CPA can work in either the even or the odd modes. For the even mode, the two beams are in phase and $\Delta = \varphi_R - \varphi_L = 0$, and the thickness L satisfies the relation $n_2 L = m\lambda_0$, where m is an integer. For the odd mode, the two beams are out of phase and $\Delta = \varphi_R - \varphi_L = \pi$, and the thickness L satisfies the relation $n_2 L = (m + \frac{1}{2})\lambda_0$, where m is an integer.

In both cases, $A_{\text{Left}}^{(\text{total})}$ is

$$A_{\text{Left}}^{(\text{total})} = \frac{\varepsilon^{(i)} e^{i\varphi_L} \left[(1 - e^{-\delta_2}) r + tt' e^{-\frac{\delta_2}{2}} \right]}{1 - r^2 e^{-\delta_2}}. \tag{12}$$

If the numerator goes to zero, the outgoing light is completely extinguished and the device behaves as a CPA. This requires

$$-(1 - e^{-\delta_2}) r = tt' e^{\frac{-\delta_2}{2}} = (1 + rr') e^{\frac{-\delta_2}{2}}. \tag{13}$$

The solution for Eq. (13) is

$$\delta_2 = \delta_{20} = -2 \ln(-r) = 2 \ln\left(\frac{n_2 + n_1}{n_2 - n_1} \right). \tag{14}$$

By substituting δ_{20} with $\frac{i4\pi n_{2i} L}{\lambda_0}$, this result is identical to Eq. (9) in [3].

Because of the symmetry, the total amplitude $A_{\text{Right}}^{(\text{total})}$ at the right surface also vanishes as $A_{\text{Left}}^{(\text{total})}$ vanishes.

The above analysis shows an important result that a slab with a complex refractive index $\tilde{n}_2$ and thickness L becomes a CPA operating in the even or odd modes when the absorption coefficient δ_2 exactly equals δ_{20}, which is given by Eq. (14). The required δ_{20} as a function of the refractive index n_2, assuming $n_1 = 1$, is shown in Fig. 2. Also shown are the corresponding ordinate scale for the required values of the imaginary part of the refractive index $n_{2i}\left(= \frac{\lambda_0 \delta_{20}}{4\pi L}\right)$ for $L =$ 100 μm and $\lambda = 945.3$ nm. The nearly vertical dashed curve is the complex refractive index of Si, and the intersection of these two curves is the operating point of a silicon-based CPA. The conditions for λ_2 as defined in Eq. (14) and plotted in Fig. 2 are identical to the key results of Eq. (9) and Fig. 2 in [3]. However, the required λ_{20} in our analysis is a critical value, rather than a threshold as defined in laser physics, because the two curves in Fig. 2 have only one intersection. If δ_{20} were a threshold, as $\delta_2 < \delta_{20}$, the device would not be a perfect absorber, and as $\delta_2 > \delta_{20}$, the device would always be a perfect absorber and vice versa. However, our analysis shows that the device is a perfect absorber only when $\delta_2 = \delta_{20}$ and, when δ_2 deviates from δ_{20}, either $\delta_2 < \delta_{20}$ or $\delta_2 > \delta_{20}$, the device ceases to be a perfect absorber.

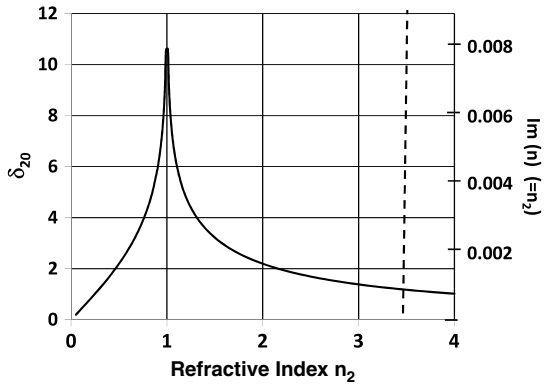

Fig. 2. Condition for perfect absorption expressed as δ_{20} and n_{2i} as a function of n_2 in a two-beam CPA. The dashed line is the n_{2i} versus n_2 relation for silicon. The intersection of these two curves is the operating point of a silicon-based CPA.

As an example, we consider a slab with $n_2 = 3.6$ immersed in air with $n_1 = 1.0$. Two coherent beams are incident on the opposite surfaces of the slab. The required δ_{20} according to Eq. (14) is calculated to be $\delta_{20} = 1.141$, or, equivalently, an imaginary part of the refractive index $n_{2i} = 0.00091$, for a slab thickness of 100 μm and wavelength of $\lambda_0 = 1.0$ μm. When $\delta_2 = \delta_{20} = 1.141$, the slab behaves as a CPA and completely extinguishes both incident coherent beams. The power output ratio, defined as the ratio of the total output versus the total power input, is

$$Q_{\text{total}}^2 = \frac{|A_{\text{Left}}^{(\text{total})}|^2 + |A_{\text{right}}^{(\text{total})}|^2}{|A_L^{(i)}|^2 + |A_R^{(i)}|^2}. \tag{15}$$

To achieve an absorption of 99.999% or a power output ratio of 10^{-5}, the value of δ_2 must fall within the range

$$\delta_2 = 1.141^{+0.0077}_{-0.0074}. \tag{16}$$

If the thickness of the slab is 100 μm and $n_{2i} = 0.00080$, the δ_2 value is 1.0, which deviates from δ_{20}, and the power output ratio is 0.004, corresponding to an absorption of 99.6%. The dependency of the power output ratio Q^2 as a function of δ_2 in the vicinity of δ_{20} is shown in Fig. 3. The results shown here are comparable with the experimental results presented in [4] if the uncertainty in the n_{2i} values deduced from published experimental data and the experimental accuracy in [4] are taken into account.

As the phase difference between two incident beams deviates from $m\pi$, the power output ratio Q^2 varies periodically from 0% to 73.5%, as shown in Fig. 4.

Chong *et al.* [3] pointed out that, "In S-matrix picture lasing occurs when a pole of the S matrix is pulled "up" to the real axis by including gain as a negative imaginary part of the refractive index. This viewpoint suggests the possibility of the time-reversed process of lasing at threshold," and "a specific degree of dissipation ("loss medium") is added to the resonator, corresponding to a positive imaginary refractive index equal in absolute value to that at the lasing threshold."

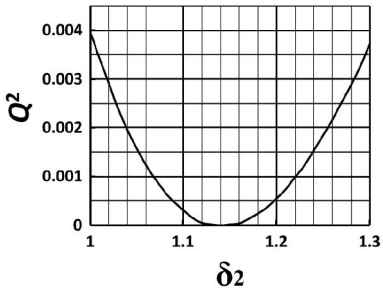

Fig. 3. Power output ratio Q^2 as a function of δ_2 for a two-beam CPA.

Wan *et al.* [4] further state that, "Reaching the precise CPA condition of perfect absorption requires tuning two parameters (e.g., n_1 and n_2 or n_2 and λ); by analogy to the laser, the CPA must have the correct absorption to reach "threshold." The "threshold" is given in Eq. (9) in [3].

Our approach is solely based on electrodynamics. The problem of the two-beam CPA is reduced to a problem of complete suppression of reflections in a Fabry–Perot interferometer through "index matching" among the media. The concept of "time reversal" used in the *S*-matrix analysis of Chong *et al.* does not exist in our analysis. The superposition of waves and index matching, commonly used in treating layered structures in optics, provides a clear and physically intuitive picture for the principle of operation of these devices and is also much easier for a device designer to follow without going through the more complex theory. Our analysis shows that reaching the precise CPA condition of perfect absorption requires tuning two parameters (e.g., n_1 and n_2 or n_2 and λ) to satisfy a well-defined relation of Eq. (14), which gives the same result as Eq. (9) and Fig. 2 in [3]. Furthermore, our analysis shows that the perfect absorption only occurs at an exact absorption coefficient, which is a critical point rather than the threshold value as defined in laser physics.

In summary, the two-beam CPA is essentially a Fabry–Perot interferometer having two coherent beams incident on two opposite surfaces of the interferometer. Our analysis based on classical electrodynamics shows that if the thickness of the slab meets the resonant condition, the two beams have a phase difference of 0 or π, and the real and imaginary parts of the refractive indices satisfy a well-defined relation given in Eq. (14), the interferometer functions as a two-beam CPA.

3. ONE-BEAM CPA

The analysis presented in the previous section can also be applied to a one-beam CPA, which is similar to the configurations of the asymmetric Fabry–Perot etalon and resonant-enhanced photodetector previously reported in [10,11]. Figure 5 shows the structure of a one-beam CPA, which consists of an absorbing medium with parallel surfaces and a total reflector on the back surface. The medium has a complex refractive index $\tilde{n}_2 = n_2 + in_2$ and a thickness L immersed in a nonabsorbing medium with a real refractive index n_1.

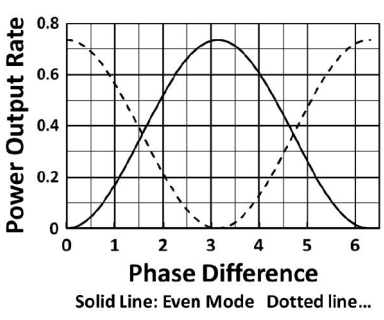

Fig. 4. Power output ratio Q^2 as a function of detuning from perfect absorption for a two-beam Fabry–Perot interferometer.

The electric field of the incident beam $I^{(i)}$ of wavelength λ_0, and frequency ω, polarized in the X direction incident on the left surface of the interferometer can be expressed as

$$E^{(i)} = A^{(i)} e^{-i(\omega t - kz)}, \tag{17}$$

where $A^{(i)}$ is the amplitude of the electric field $E^{(i)}$.

On the right surface, there is a phase shift upon reflection from the total reflector and the complex reflection coefficient can be expressed as $\tilde{r}'' = r'' e^{i\theta}$, where θ can be a value between 0 and π, depending on the thicknesses and refractive indices of the coating layers of the total reflector.

Considering multiple reflections of the incident beam in the interferometer, the superposition of the reflected beams results in an amplitude of the reflected beam given by

$$\begin{aligned} A^{(r)} &= (r + t\tilde{r}''t'e^{i\delta} + t\tilde{r}''r'\tilde{r}''t'e^{i2\delta} + \ldots)A^{(i)} \\ &= \left(r + \frac{t\tilde{r}''t'e^{i\delta}}{1 - r'\tilde{r}''e^{i\delta}}\right)A^{(i)} = \frac{r + \tilde{r}''e^{i\delta}}{1 - r'r''e^{i\delta}}A^{(i)}. \end{aligned} \tag{18}$$

The amplitude reflection coefficient D is defined as

$$D = \frac{A^{(r)}}{A^{(i)}} = \frac{r + \tilde{r}''e^{i\delta_1 - \delta_2}}{1 - r'\tilde{r}''e^{i\delta_1 - \delta_2}}. \tag{19}$$

For a CPA, the numerator in Eq. (19) should be zero. If $n_1 = 1$ in air and r is negative in most cases, $r''e^{i(\theta+\delta_1)}$ must be positive and real. This condition can be met by requiring $\theta + \delta_1 = 2m\pi$. Under these conditions, $\tilde{r}'' = 1$ and the amplitude reflection coefficient D becomes

$$D = \frac{A^{(r)}}{A^{(i)}} = \frac{r + e^{-\delta_2}}{1 - r'e^{-\delta_2}}. \tag{20}$$

To be a CPA, the numerator must vanish, which requires

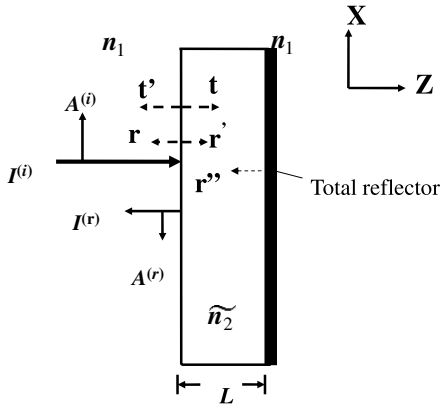

Fig. 5. Fabry–Perot interferometer with a single beam incident on the left surface.

$$\delta_2 = \delta_{20} = -\ln(-r) = \ln\left[\frac{(n_2+n_1)}{(n_2-n_1)}\right]. \tag{21}$$

For some total reflectors, such as metallic films, which are absorptive, r'' may be slightly less than 1. In such a case, vanishing of the numerator requires

$$\delta_2 = \delta_{20} = -\ln\left(-\frac{r}{r''}\right) = \ln\left[r''\frac{(n_2+n_1)}{(n_2-n_1)}\right]. \tag{22}$$

It shows that for a given material with a complex refractive index $\tilde{n}_2$ immersed in a medium with a real refractive index n_1, a CPA requires that the absorption coefficient δ_2 equal δ_{20} given in Eq. (21) for dielectric coating and Eq. (22) for metallic coating. Figure 6 shows the required δ_{20} as a function of n_2 based on Eq. (22) and when $n_1 = 1$ and $r'' = 1$.

If δ_2 deviates from δ_{20}, the output will not be completely extinguished. For example, assuming $n_2 = 3.4$, $r'' = 1$, and a power output ratio Q^2 defined as $Q^2 = \frac{|A^{(r)}|^2}{|A^{(i)}|^2}$, the plot of Q^2 as a function of δ_2 is shown in Fig. 7.

In summary, a one-beam CPA requires that the thickness L meet the condition $\theta + \delta_1 = 2m\pi$ and the real and imaginary parts of the refractive index, n_2 and n_{2i}, of the medium satisfy the relation $\delta_2 = \delta_{20}$ as defined in Eq. (22).

4. THREE-STATE PHASE-CONTROLLED DIRECTIONAL OPTICAL SWITCH

The two-beam interferometer can be configured to work as a three-state phase-controlled optical switch to produce three output states and their complementary states from the two output ports by controlling the relative phase of the input beams. The analysis is identical to that of the two-beam coherent interferometer except that the thickness of the two-beam Fabry–Perot interferometer satisfies the relation $n_2 L = (m + \frac{1}{4})\lambda_0$, where m is an integer. From Eqs. (10) and (11), this relation leads to leads to $e^{i\delta_1} = -1$, $e^{i\delta} = -e^{-\delta_2}$, $e^{i\frac{\pi}{2}} = e^{i\frac{\pi}{2}}$, and $e^{i\frac{\delta}{2}} = e^{i\frac{\pi}{2}-\frac{\delta_2}{2}}$.

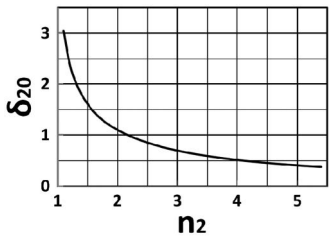

Fig. 6. Condition for perfect absorption expressed in δ_{20} as a function of n_2 in a one-beam Fabry–Perot interferometer.

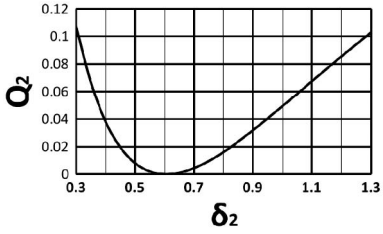

Fig. 7. Power output ratio Q^2 as a function of δ_2 for a one-beam CPA in the vicinity of perfect absorption.

$$A_{\text{Left}}^{(\text{total})} = \frac{\varepsilon^{(i)}e^{i\varphi_L}[(1+{}_e{-}\delta_2)r + tt'e^{i\frac{\pi}{2}-\frac{\delta_2}{2}}e^{i\Delta}]}{1+r^2e^{-\delta_2}}, \tag{23}$$

$$A_{\text{right}}^{(\text{total})} = \frac{\varepsilon^{(i)}e^{i\varphi_R}[(1+e^{-\delta_2})r + tt'e^{i\frac{\pi}{2}-\frac{\delta_2}{2}}e^{-i\Delta}]}{1+r^2e^{-\delta_2}}. \tag{24}$$

When the phase difference Δ satisfies the relation $\Delta = \varphi_R - \varphi_L = -\frac{\pi}{2}$, then

$$A_{\text{Left}}^{(\text{total})} = \frac{\varepsilon^{(i)}e^{i\varphi_L}[(1+e^{-\delta_2})r + tt'e^{-\frac{\delta_2}{2}}]}{1+r^2e^{-\delta_2}}. \tag{25}$$

The outgoing beam from the left, $A_{\text{Left}}^{(\text{total})}$, vanishes when the numerator is zero, which requires

$$e^{-\frac{\delta_2}{2}} = \frac{tt' \pm \sqrt{(tt')^2 - 4R}}{2\sqrt{R}}. \tag{26}$$

Using Eqs. (3) and (4), this relation can be expressed in terms of the real part of the refractive index of the interferometer medium n_2 as

$$\delta_{20} = -2\ln\left(\frac{2+\sqrt{3n_2^2+2n_2^2-1}}{2(n_2^2-1)}\right), \tag{27}$$

where $R = -rr'$. The values of δ_{20} plotted as a function of n_2 are shown in Fig. 8.

However, under this condition, the outgoing beam from the right surface

$$A_{\text{Right}}^{(\text{total})} = \frac{\varepsilon^{(i)}e^{i\varphi_L}[(1+e^{-\delta_2})r - tt'e^{-\frac{\delta_2}{2}}]}{1+r^2e^{-\delta_2}} \tag{28}$$

never vanishes because the term $[(1+e^{-\delta_2})r - tt'e^{-\frac{\delta_2}{2}}]$ is always negative, and never goes to zero. Under this condition $A_{\text{Right}}^{(\text{total})}$ becomes

$$A_{\text{Right}}^{(\text{total})} = \frac{\varepsilon^{(i)}e^{i\varphi_L}[(1+e^{-\delta_{20}})r - tt'e^{-\frac{\delta_{20}}{2}}]}{1+r^2e^{-\delta_{20}}} = \frac{2\varepsilon^{(i)}e^{i\varphi_L}(1+e^{-\delta_{20}})r}{1+r^2e^{-\delta_{20}}}, \tag{29}$$

and the power output ratio is

$$Q_{\text{Right}}^2 = \frac{|A_{\text{Right}}^{(\text{total})}|^2}{2|\varepsilon^{(i)}|^2} = \frac{1}{2}\times\left[\frac{2(1+e^{-\delta_{20}})r}{1+r^2e^{-\delta_{20}}}\right]^2. \tag{30}$$

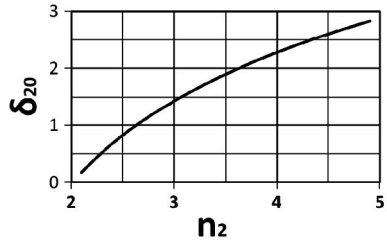

Fig. 8. Condition expressed as δ_{20} as a function of n_2 for a two-beam Fabry–Perot interferometer to produce zero output on one surface and nonzero output on the other.

When Δ is tuned to the value $\Delta = \varphi_R - \varphi_L = \frac{\pi}{2}$, the output levels from the two surfaces are reversed; i.e., at $\delta_2 = \delta_{20}$, the outgoing beam at the right surface vanishes, and at the left surface

$$Q^2_{\text{Left}} = \frac{|A^{(\text{total})}_{\text{Left}}|^2}{2|\varepsilon^{(i)}|^2} = \frac{1}{2} \times \left[\frac{2(1+e^{-\delta_{20}})r}{1+r^2e^{-\delta_{20}}}\right]^2 \tag{31}$$

is nonzero.

When Δ is tuned to the value $\Delta = \varphi_R - \varphi_L = 0$,

$$A^{(\text{total})}_{\text{Left}} = A^{(\text{total})}_{\text{Right}} = \frac{\varepsilon^{(i)}e^{i\varphi_L}[(1+e^{-\delta_{20}})r + tt'e^{i\frac{\pi}{2}-\frac{\delta_{20}}{2}}]}{1+r^2e^{-\delta_{20}}} \tag{32}$$

Since $\delta_2 = \delta_{20}$, $(1+e^{-\delta_2})r = tt'e^{-\frac{\delta_2}{2}}$, we have

$$A^{(\text{total})}_{\text{Left}} = A^{(\text{total})}_{\text{Right}} = \frac{\varepsilon^{(i)}e^{i\varphi_L}(1+e^{-\delta_{20}})r(1+i)}{1+r^2e^{-\delta_{20}}}, \tag{33}$$

$$Q^2_{\text{Left}} = Q^2_{\text{right}} = \frac{|A^{(\text{total})}_{\text{Left}}|^2}{2|\varepsilon^{(i)}|^2} = \frac{|A^{(\text{total})}_{\text{Right}}|^2}{2|\varepsilon^{(i)}|^2} = \left[\frac{(1+e^{-\delta_{20}})r}{1+r^2e^{-\delta_{20}}}\right]^2. \tag{34}$$

The output power ratios from the two end surfaces are equal. As an example, assuming $n_2 = 3.4$, $n_1 = 1.0$, then $\delta_{20} = 1.811$. If the phase difference Δ is tuned to the value $\Delta = \varphi_R - \varphi_L = -\frac{\pi}{2}$, the power output ratios from the left and right surfaces are

$$Q^2_{\text{Left}} = 0, \tag{35}$$

$$Q^2_{\text{Right}} = \frac{|A^{(\text{total})}_{\text{Right}}|^2}{2|\varepsilon^{(i)}|^2} = \left[\frac{2(1+e^{-\delta_{20}})r}{1+r^2e^{-\delta_{20}}}\right]^2 = 0.7352. \tag{36}$$

As Δ is tuned to $\Delta = \varphi_R - \varphi_L = \frac{\pi}{2}$, the power output ratios are

$$Q^2_{\text{Right}} = 0, \tag{37}$$

$$Q^2_{\text{Left}} = \frac{|A^{(\text{total})}_{\text{Right}}|^2}{2|\varepsilon^{(i)}|^2} = \left[\frac{2(1+e^{-\delta_{20}})r}{1+r^2e^{-\delta_{20}}}\right]^2 = 0.7352. \tag{38}$$

When Δ is tuned to be $\Delta = \varphi_R - \varphi_L = 0$, the power output ratios are

$$Q^2_{\text{Right}} = Q^2_{\text{Left}} = \frac{|A^{(\text{total})}_{\text{Right}}|^2}{2|\varepsilon^{(i)}|^2} = \frac{|A^{(\text{total})}_{\text{Left}}|^2}{2|\varepsilon^{(i)}|^2}\left[\frac{(1+e^{-\delta_{20}})r}{1+r^2e^{-\delta_{20}}}\right]^2 = 0.3676. \tag{39}$$

The above calculation shows that when the thickness L of the two-beam Fabry–Perot interferometer satisfies the relation $n_2L = (m+\frac{1}{4})\lambda_0$, where m is an integer, the device functions as a three-state optical switch that provides three output states. The output of the device can be made to switch among these three states by controlling the phase of either the left or the right beam. The device can also be configured as a directional switch to produce fully off (zero) or fully on states on one of the surfaces and a complementary output on the other surface. Such a device may be used in computation based on the trinary number system. The controlling signal and output states are summarized in Table 1.

Table 1. Working Chart of the Three-State Optical Switch

State	Phase difference Δ	Channel A (Outgoing beam at left surface)	Channel B (Outgoing beam at right surface)
A	$\Delta = -\pi/2$	Off (0)	On (0.735)
B	$\Delta = 0$	On (0.368)	On (0.368)
C	$\Delta = +\pi/2$	On (0.735)	Off (0)

5. SUMMARY

In this paper, we have analyzed the one- and two-beam CPAs and the three-state phase-controlled optical switch using classical electrodynamics by considering the superposition of waves after multiple reflections in a Fabry–Perot interferometer. The results show that for the CPAs, the incident beam(s) must have correct phases and amplitudes, and the real and imaginary parts of the refractive indices of the medium in the interferometer must satisfy a well-defined relation. Our results are in agreement with those obtained using the *S*-matrix analysis. Further analysis shows that the two-beam device can also function as a three-state phase-controlled and directional optical switch, which can be controlled by tuning the relative phase of one of the incident beams.

Our entire analysis is based on the principle of superposition of transmitted and reflected waves, which is the standard optics approach for analyzing multilayered structures for suppressing reflections. The total suppression of reflection, and thus total absorption, is achieved through "index matching" by tailoring the layer thickness to the complex refractive indices of the media. The concept of index matching in a layered structure to minimize reflections (and thereby to maximize absorptions) provides a clear and physically intuitive picture for the principle of operation of CPAs. The approach is also much easier for device designer to follow without going through a more complex theory. Our analysis also shows that the perfect absorption only occurs at an exact absorption coefficient, which is a critical point rather than a threshold value as defined in laser physics.

ACKNOWLEDGMENTS

This work was supported by grants from the National Center for Research Resources (G 12 RR003037) and the National Institute on Minority Health and Health Disparities (8 G12 MD 007599) from the National Institutes of Health.

REFERENCES

1. C. F. Gmachl, "Laser science: suckers for light," Nature **467**, 37–39 (2010).
2. S. Longhi, "Backward lasing yields a perfect absorber," Physics **3**, 61 (2010).
3. Y. Chong, L. Ge, H. Cao, and A. Stone, "Coherent perfect absorbers: time-reversed lasers," Phys. Rev. Lett. **105**, 053901 (2010).
4. W. Wan, Y. Chong, L. Ge, H. Noh, A. D. Stone, and H. Cao, "Time-reversed lasing and interferometric control of absorption," Science **331**, 889–892 (2011).
5. T. H. Maiman, "Stimulated optical radiation in ruby," Nature **187**, 493–494 (1960).
6. E. L. Hahn, "Spin echoes," Phys. Rev. **80**, 580–594 (1950).
7. I. D. Abella, N. A. Kurnit, and S. R. Hartmann, "Photo echos," Phys. Rev. **141**, 391–406 (1966).
8. H. S. Tsien, *Engineering Cybernetics* (McGraw-Hill, 1954).
9. M. Born and E. Wolf, *Principle of Optics*, 7th ed. (Cambridge University, 1999), pp. 360–362.
10. K. Kishino, S. Unlu, J. Chyi, J. Reed, L. Arsenault, and H. Morkoc, IEEE J. Quantum Electron. **27**, 2025–2034 (1991).
11. J. F. Heffnan, M. H. Moloney, J. Hegarty, J. S. Roberts, and M. Whitehead, "All optical high contrast absorptive modulation in asymmetric Fabry-Perot etalon," Appl. Phys. Lett. **58**, 2877 (1991).